Brain tissue pulsation in healthy volunteers

P Turner[1,2*], C Banahan[1,3*], M Alharbi[1], J Ince[1], S Venturini[1], S Berger[1], I Bnini[1], J Campbell[1], KW Beach[4], M Horsfield[5], M Oura[6], A Lecchini-Visintini[2], and EML Chung[1,3,7]

[1] Department of Cardiovascular Sciences, University of Leicester, UK

[2] Department of Engineering, University of Leicester, UK

[3] Department of Medical Physics, University Hospitals of Leicester NHS Trust, UK

[4] University of Washington, Seattle WA, USA

[5] Xinapse Systems, UK

[6] Nihon Kohden, Tokyo, Japan

[7] Leicester Cardiovascular Biomedical Research Centre, UK

[*] Joint first authors

Correspondence: Dr Emma Chung, Department of Cardiovascular Sciences, University of Leicester, RKCSB, Leicester Royal Infirmary, LE1 7RH, UK

Email: emlc1@le.ac.uk

Tel: +44 (0)116 252 5839

Abstract

It is well known that the brain pulses with each cardiac cycle, but interest in measuring cardiac-induced brain tissue pulsations (BTPs) is relatively recent. This study aimed to generate BTP reference data from healthy subjects for future clinical comparisons, and to model BTPs measured through the forehead and temporal positions as a function of age, sex, heart rate, mean arterial pressure, and pulse pressure. A multivariate regression model was developed based on transcranial tissue Doppler BTP measurements from 107 healthy adults (56 male) aged from 20 to 81 years. A subset of 5 participants (aged 20 to 49 years) underwent a brain MRI scan to relate the position of the ultrasound beam to anatomy. BTP amplitudes were found to vary widely between subjects (from ~4 to ~150 μm), and were strongly associated with pulse pressure. Comparison with MR images confirmed regional variations in BTP with depth and probe position.

Word Count (149/150)

Key words: Transcranial Tissue Doppler, ultrasound, healthy volunteers, brain tissue pulsations, brain tissue displacement, brain MRI

Introduction

As can be seen through the fontanelle of newborn infants, and in patients undergoing neurosurgery, the brain visibly pulsates over the cardiac cycle. Regional pulsations of brain tissue are thought to be strongly influenced by propagation of arterial pulsations into surrounding tissue and variations in brain tissue compliance. The characteristics of these pulsations are also influenced by damping, due to the brain being confined within the skull, tethering of the brain to other structures, and a balance between tissue, vasculature, and cerebrospinal fluid (CSF) compartmental volumes over the cardiac cycle (described by the Monroe Kellie doctrine) (Greitz et al. 1992). Although Doppler techniques have been applied to characterise cardiac tissue motion for many years (Ommen et al. 2000), the application of Doppler ultrasound to measurement of brain tissue motion is relatively unexplored. The aim of this study was to provide the first estimates of brain tissue motion for a wide cross-section of healthy adults.

Our existing knowledge of brain tissue motion comes predominantly from MRI studies. Weaver et al. (2012) showed that it was possible to measure and model tissue strain over the cardiac cycle to estimate brain tissue elasticity. Weaver quantified intrinsic pulsations of brain tissue relative to their proximity to the circle of Willis. Pulsation amplitude was estimated for 4 regions of the brain, in 6 volunteers. Pulsations were found to be strongest in tissue surrounding the circle of Willis (~150 μm) and weakest at the brain's periphery (~10 μm). One study showed that the volume of white matter hyperintensities in 9 subjects, detected using MRI, correlated with decreased pulsation amplitude measured using a phased array ultrasound probe (Ternifi et al. 2014). Most recently, Terem et al. (2018) developed a method of amplifying brain motion from a gated cine MRI scan, called amplified MRI (aMRI). This aMRI technique revealed clear differences in brain tissue motion between a healthy volunteer and a patient with a Chiari I malformation, suggesting that measurement

of brain tissue motion may be used clinically to study changes in brain tissue displacement associated with pathology.

Mosher et al. (2020) used measurements of brain tissue motion associated with the cardiac cycle, obtained using electrodes, to identify different cell types in the brain. Findings from this study suggested that the amplitude of brain motion is significantly stronger in deep brain structures compared to amplitudes in the cortex. Previous ultrasound studies have used a phased array ultrasound imaging probe, more commonly used for echocardiography, to map brain tissue motion. A recent study investigates the concept of using B-mode ultrasound imaging to quantify BTPs in a 2D region of interest, with the technique being validated using a phantom, an elderly subject, and a patient with Alzheimer's disease (Jurkonis et al. 2020).

The majority of ultrasound studies use a technique called Tissue Pulsatility Imaging (TPI). TPI studies have been summarised in a systematic review (Ince et al, 2019) and suggest that brain tissue pulsations could be used as a potential marker for brain pathology and impaired cerebral haemodynamics. An increase in BTP amplitude was observed in the visual cortex of a healthy volunteer presented with a visual stimulus (Kucewicz et al. 2007). BTPs were also studied in healthy participants during a period of hyperventilation, and it was found that both CO_2 levels, and BTP amplitude significantly decreased during the protocol (Kucewicz et al, 2008). Recently, a TPI study looking into the impact of music on BTPs found that pulsations of 25 healthy volunteers were significantly reduced when listening to relaxing music (Siragusa et al. 2020).

Numerous TPI studies have investigated BTPs in patients with diagnosed pathology. For instance, it was found that elderly patients diagnosed with both depression and diabetes experienced significantly weaker pulsations than those only diagnosed with diabetes (Desmidt et al. 2011). However, a later study investigating mid-life females with depression observed contradictory results, suggesting a significant increase in pulsations of those with

depression compared to control subjects and those in remission (Desmidt et al. 2017). One study, investigating BTP changes in 22 elderly subjects with orthostatic hypotension (OH), found that mean brain tissue pulsatility (representing global intracranial pulsatility) was significantly weaker in patients with OH compared to control subjects without OH (Biogeau et al. 2017). Although previous studies have identified statistically significant differences between patients and control groups, these results need to be interpreted with caution. It is important to establish the true extent of variability in BTPs amongst the healthy population to inform sample size calculations and ensure studies include sufficient participants, confidently identify differences, and avoid type 1 statistical errors.

Transcranial Tissue Doppler (TCTD) is a novel technique introduced in this study; it differs to the previous studies described above, which use tissue pulsatility imaging (TPI). TPI uses a phased-array ultrasound probe (typically used in echocardiography) to map brain tissue motion in a 2D region of interest. The TCTD technique we introduce in this paper uses a small, wearable, single-element ultrasound probe. An advantage of TCTD measurement of BTPs is that measurements can be obtained from any position on the head; the probe is light enough to wear, and measurements do not require a skilled operator.

The aim of this study was to provide normative data characterising variations in tissue displacement measured using TCTD across a wide cross-section of healthy adults. An exploratory statistical analysis is performed to summarise the range of pulsations seen in healthy subjects, and to model BTPs measured through the forehead and temporal position as a function of Age, Sex, heart rate (HR), mean arterial pressure (MAP), and pulse pressure (PP). Ultrasound measurements are complemented by MR images in five volunteers to aid the interpretation of pulsation waveforms in relation to brain anatomy.

Materials and Methods

Subjects

Adults with no previous history of brain injury were recruited to this study following a protocol approved by the University of Leicester, Medicine and Biological Sciences Research Ethics Committee. Participants were recruited through online and email advertising to staff and student groups within the University of Leicester. To provide a good spread of ages, working age participants were also recruited with the co-operation of a local business (Cloudcall Ltd., UK) who advertised the study to their employees and allowed interested staff to take part during working hours. Volunteers aged over 65 years were recruited with the assistance of our local branch of the University of the Third Age (an international network of learning groups aimed towards older people), who included an advert for our study in their newsletter. All participants provided written informed consent.

Ultrasound Beam Characterisation

The dimensions of the ultrasound beam were investigated using an in-house beam plotting system, comprising a hydrophone needle (Precision Acoustics Ltd., UK) submerged in a water tank. The needle was moved across the x, y, and z directions of the ultrasound beam using a mechanical stage, and was used to measure the intensity of the beam at a number of specified locations. The ultrasound beam was found to have a consistent narrow width along the length of the beam, with a Full Width at Half Maximum (FWHM) ranging from 2.7 mm at a depth of 5 cm, to a maximum width of 3.6 mm at a depth of 7 cm. The approximate path of the ultrasound beam within the brain for the temporal probe position can be found in Figure 1, along with an illustration of the TCTD equipment setup. It should be noted that the shape and direction of the beam profile is likely to be modified during TCTD recordings due to the beam passing through the skull, therefore the beam plot shown in

Figure 1 is only indicative and may not represent the exact path of the ultrasound beam within the brain.

MRI Protocol and Analysis

In order to better understand the impact of brain anatomy on BTP signals, an additional 5 participants (3 male, median age: 22 years, range: 20 – 49 years) underwent magnetic resonance imaging (MRI) to image the brain and arteries. The transducer was attached to a head frame so that the path of the beam through the head could be estimated and fiducials (oil filled capsules) were attached to the head to act as landmarks that would be visible on the MRI scan, see Figure 1a. Participants then underwent brain imaging using a 3T MR scanner (Magnetom Skyra; Siemens Medical, Erlangen, Germany). The scans included a 3-plane localizer, 3D T1-weighted sagittal and time-of-flight magnetic resonance angiography (MRA). The T1-weighted slices were resampled using 3D multi-planar reconstruction (Jim, Xinapse Systems, UK) to visualise a plane through the dataset containing the ultrasound beam path, using the oil capsule fiducials as a guide.

TCTD Protocol and Data Acquisition

Participants completed a health questionnaire recording prescribed medications and current health conditions. Participants reporting any acute or chronic medical conditions were excluded. Participants had their brachial blood pressure measured using a standard arm-cuff device (OMRON Healthcare UK Ltd., UK). Blood pressure measurements were repeated at the start and end of each recording session to provide an average value for statistical analysis. Participants were asked to wear a 3-lead ECG monitor (Nihon Kohden, Japan) to record the timing of the pulsations relative to the QRS of each cardiac cycle. Participants were seated in

an upright position, and were asked to close their eyes and remain still during each measurement to avoid generating motion artefacts.

Ultrasound recordings were obtained using a modified Spencer Technologies (Seattle, WA) Transcranial Doppler (TCD) system (8 kHz PRF, M-mode, 33 Doppler gates), equipped with a 2 MHz transducer. The transducer was held in place using an elasticated headband and custom probe holder. For each participant, TCTD data were recorded from 4 probe positions: through the left and right temporal windows, and through the forehead above the centre of each eyebrow. As a commercially available TCD system was modified for recording brain tissue pulsations during this study, it was not possible to view the data at the time of acquisition. Therefore, the quality of the data could only be determined after post-processing and analysis. For this reason, two measurements were recorded from each probe position (left temporal, left forehead, right temporal, right forehead), and the recording least affected by artefacts was taken forward for further analysis, resulting in a maximum of 4 recordings being analysed for each participant. Artefacts were typically caused by movement of the head (e.g. coughing, blinking, or probe motion).

Each ultrasound recording was 8 seconds long, providing tissue motion data from 33 overlapping 3 mm sample depths (or gates) spaced 2 mm apart. Sample depths ranged from 22 to 86 mm, however, data from the last 3 gates (82 - 86 mm) were discarded due to increased signal noise. Ultrasound recordings were synchronised to ECG data and analysed using software developed in MATLAB (The MathWorks, Inc., United States).

TCTD Signal Processing

The in-phase and quadrature-phase (IQ) data from each 8 second recording were down-sampled from 8 kHz to 160 Hz to reduce the size of our files, giving a temporal resolution of 6.25 ms. Tissue velocity at each depth was estimated using an autocorrelator (Hoeks et al.

188 1994) and integrated over time to obtain a BTP signal representing real-time tissue
189 displacement at each depth. The BTP signals were then filtered to remove respiration using a
190 high pass filter with cut-off at 75% of the mean cardiac cycle frequency. Heart rate was
191 estimated by calculating the mean cardiac frequency using each subject's ECG R-wave
192 interval.

193 The BTP signals were displayed in MATLAB, and manually inspected, with the R-R
194 intervals overlaid, to allow the user to remove any cardiac cycles containing artefacts. Further
195 analysis was based on these cleaned (artefact free) data. Artefacts were defined as any
196 noticeable perturbations not regularly repeating with the cardiac cycle. Example BTP signals
197 are shown in Figure 2.

198 In general, over each R-R interval, the tissue is initially moving outwards towards the
199 transducer. The tissue then moves sharply inward, away from the transducer for
200 approximately 25% of the cardiac cycle, and then relaxes by moving outward again for the
201 remainder, and for the initial part of the next cardiac cycle. For most brain regions the peak
202 consistently preceded the trough, however, for some recordings, BTP signals at different
203 depths moved in opposite directions (see Figure 3) and the timing of the peak and trough
204 were reversed.

205 The analyses presented in this work focus on quantifying typical amplitudes of BTP
206 signals. For each recording, the BTP Amplitude at each depth was calculated as the average
207 of the maximum displacement (i.e. the absolute difference between the peak and trough of
208 each cardiac cycle – as illustrated in Figure 2c). For each recording, a Bulk BTP signal was
209 also calculated as the average of the BTP signals across all 30 depths, representing collective
210 displacement of the brain over the cardiac cycle. For each Bulk BTP signal the Bulk BTP
211 Amplitude was then calculated.
212

213 Statistical Analysis

214 Statistical analysis of demographic and BTP features were performed in MATLAB.
215 As the BTP Amplitude distribution was skewed toward lower values (i.e. non-normally
216 distributed), and since variances were observed to increase with amplitude, data were log-
217 transformed prior to modelling. The resulting log-transformed distribution was confirmed to
218 be normally distributed. Paired and two sample t-tests were then carried out on log-
219 transformed Bulk BTP Amplitude data to assess whether pulsations differed with probe
220 position. Stata v.15 (StataCorp LLC) was used to develop a multivariate regression model to
221 explore the effects of Age, Sex, PP, MAP, and HR on Bulk BTP Amplitude (section:
222 Multivariate Regression Model).

223

224 # Results

225 MRI Results

226 In the 5 subjects who underwent MRI, BTPs were studied alongside the
227 corresponding brain structure visualised using T1-weighted MRI. From these data, variations
228 in BTP waveform features with depth were related to regional variations in brain anatomy.

229 Two examples, from a 22 year old male and 20 year old female, are provided in
230 Figure 3. In the case of the 22 year old male volunteer - Figure 3(a) - the associated T1-
231 weighted MRI shows the ultrasound beam entering the frontal cortex within the frontal lobe,
232 passing from white to grey matter at 36 mm, moving from the frontal cortex to the corpus
233 callosum at 40 mm and from the corpus callosum into the ventricles at 68 mm. In the case of
234 the 20 year old female volunteer - Figure 3(b) - the MRI shows the beam passing through a
235 region of white matter to grey matter in the inferior frontal lobe at 30 mm, before entering the
236 anterior cingulate cortex at 40 mm and to the corpus callosum at 62 mm. In both cases, BTP

signals were well correlated in homogenous brain regions, while changes of waveform were associated with differing motion in adjacent tissue structures.

TCTD Results

A total of 107 healthy volunteers were recruited to this study, comprising 56 men and 51 women. Volunteers ranged from 20 to 81 years of age (mean age: 41 years). Out of a total of 428 independent recordings, 405 recordings were suitable for further analysis; 23 recordings were rejected due to a large number of artefacts. For the forehead positions, 96 subjects provided acceptable recordings for analysis from both the left and right hemispheres, and 105 subjects provided at least one acceptable recording. For the temporal positions, 97 subjects provided acceptable recordings from both the left and right hemispheres, and all 107 subjects provided at least one acceptable recording.

Amplitude of Tissue Displacement

Median forehead Bulk BTP Amplitude was 16.1 μm [IQR: 10.5, 22.9] for the left hemisphere and 18.4 μm [IQR: 11.6, 27.3] for the right. The median Bulk BTP Amplitude measured from the temporal positions was 8.8 μm [IQR: 5.9, 12.6] for the left hemisphere, and 9.3 μm [IQR: 6.4, 13.6] for the right hemisphere. To further investigate the nature of any potential differences in pulsation amplitude between hemispheres, the difference in Bulk BTP Amplitude (Δ Bulk BTP Amplitude) for each pair of BTP measurements was estimated by subtracting the left from the right side, see Figure 4.

A noticeable difference between hemispheres was a common occurrence. The median absolute magnitude of Δ Bulk BTP Amplitude was 8.7 μm [IQR: 3.9, 15.2] in the forehead positions and 3.8 μm [IQR: 1.6, 7.4] in the temporal positions. For the forehead positions, 59% of participants experienced stronger right brain pulsations. The median Δ Bulk BTP

Amplitude at the forehead was 2.6 μm [IQR: -5.1, 12.0]. This difference between hemispheres at the forehead was of borderline significance, based on a paired t-test using log-transformed values ($p = 0.05$). For the temporal positions, 57% of participants experienced stronger pulsations in their right hemisphere. The median Δ Bulk BTP Amplitude at the temporal positions was 0.9 μm [IQR: -3.1, 4.0]. This small difference in pulsation amplitude at the temporal positions was not found to be statistically significant, $p = 0.73$. It may be of interest in future to examine whether inter-hemispheric differences are impacted by brain dominance or cognitive tasks, but this was not the focus of the current study.

Bulk BTP Amplitude was found to be significantly higher for measurements obtained from the forehead positions than through the temporal windows, Figure 5. The median Bulk BTP Amplitude for the forehead positions was 17.0 μm [IQR: 11.3, 25.4], compared to 9.2 μm [IQR: 6.0, 12.9] from the temporal positions ($p < 0.001$ using a paired t-test on log transformed data).

BTP Amplitude increased approximately linearly with depth; weakest pulsations were typically observed from the shallower gates with strongest pulsations from the deepest gates. Median BTP Amplitude for the forehead positions increased from 10.4 μm [IQR: 7.2, 14.6], at a depth of 22 mm, to 32.4 μm [IQR: 23.1, 46.5] at 80 mm. Median BTP Amplitude for the temporal positions increased from 5.2 μm [IQR: 3.4, 7.6] at 22 mm to 17.6 μm [IQR: 11.5, 27.4] at 80 mm. Variations in BTP Amplitudes with depth, when observed through the forehead and temporal positions, are presented in Figure 6.

Multivariate Regression Model

A multivariate regression model was constructed to investigate how much of the variability seen in Bulk BTP Amplitude measurements could be explained by continuous variables, such as Age, Pulse Pressure (PP), Mean Arterial Pressure (MAP), and Heart Rate

(HR). This model was also used to explore whether there were any significant differences in Bulk BTP Amplitude between men and women. Recordings from 105 subjects, with at least one valid forehead recording and one valid temporal recording, were included in the regression analysis. For each subject, Bulk BTP Amplitude measured from equivalent probe positions on the left and ride sides were averaged if both recordings were present.

Data relating to Age, Sex, PP, MAP and HR were available for all subjects. To assess the potential for multicollinearity between variables, the variance inflation factor (VIF) for each parameter was estimated and found to be < 2.5 in all cases (Mean VIF = 1.34), suggesting collinearity was unlikely to be an issue for our model. Pearson's correlation coefficients were also calculated for all explanatory variables within the model, and only weak/moderate correlations were observed (Pearson's correlation coefficient < 0.5). Prior to inclusion in the model, PP, MAP, HR, and Bulk BTP Amplitude values were log-transformed to improve adherence to underlying statistical assumptions of normality

As a first step, a univariable analysis was carried out to explore associations between individual explanatory variables and log(Bulk BTP Amp. Fore.) and log(Bulk BTP Amp. Temp.) as outcomes. Parameters where $p > 0.1$ on univariable analysis were not modelled further. This analysis suggested that log(MAP) and log(HR) ($p = 0.50$ and $p = 0.55$ respectively) were not significant predictors of Bulk BTP Amplitude.

For the remaining explanatory variables (Age, Sex, and log(PP)), multivariable regression models featuring polynomial terms up to order 2 were considered. In order to select significant combinations of terms, 36 hierarchically well-formulated models (out of 127 possible models) were assessed following the procedure suggested by Peixoto (1987). Criteria for identifying the best model included: (1) all variables in the model had to be statistically significant for at least one of the outcome variables (log(Bulk BTP Amp. Fore.) or log(Bulk BTP Amp. Temp.)), (2) the overall model should significantly explain both

312 outcome variables, and (3) the variability in outcome parameters explained by the model (R^2
313 value) should be the highest after considering steps (1) and (2).

314 Following this plan, our preferred model included only linear terms; log(PP), Age,
315 and Sex, with an overall level of significance of $p < 0.001$ across both outcome variables. A
316 Doornik-Hansen test suggested the residuals of this reduced model did not significantly
317 deviate from a normal distribution ($p = 0.07$). Final preferred model coefficients, p-values,
318 and R^2 values are summarised in Table 1. The final model for the forehead position is:
319 $\log(\textit{Bulk BTP Amp. Fore.}) = 0.198 + 0.753 \log(\textit{PP}) - 0.004\ \textit{Age} - 0.045\ \textit{Sex}$. The final model
320 for the temporal position is: $\log(\textit{Bulk BTP Amp. Temp.}) = -0.090 + 0.597 \log(\textit{PP}) + 0.001$
321 $\textit{Age} + 0.110\ \textit{Sex}$.

322 The influence of each continuous variable on Bulk BTP Amplitude can be explained
323 in terms of small percentage increments. A 1% increase in PP is associated with a 0.8%
324 increase in Bulk BTP Amplitude for the forehead and a 0.6% increase for the temporal
325 position. For example, holding Age at a constant value of 41 years (the average value), an
326 increase in PP from 40 mmHg to 50 mmHg is predicted to be associated with an increase in
327 Bulk BTP Amplitude from 17.4 μm to 20.6 μm when measured through the forehead, and an
328 increase from 8.1 μm to 9.2 μm when measured from the temporal position.

329 Age was found to be a significant predictor of Bulk BTP Amplitude for measurements
330 made through the forehead. A 1 year increase in Age, above the age of 20, corresponded to a
331 decrease in Bulk BTP Amplitude of 0.9% for forehead BTP measurements. As an example, if
332 PP is held at the median value of 43 mmHg, an increase in Age from 20 to 80 years would be
333 associated with a decrease in Bulk BTP Amplitude from 22.3 μm to 12.8 μm. For
334 measurements made from the temporal position the effect of Age was smaller, with a non-
335 significant p-value and 95% confidence intervals that included zero.

Sex was found to be a significant factor for temporal position measurements ($p = 0.01$), with Bulk BTP Amplitude being 29% higher in men than in women. For example, adopting average values for all terms in the model, Bulk BTP Amplitude measured through the temporal position for a man would be 10.9 μm, compared to 8.4 μm for a woman. This small difference between the sexes was not confirmed in the forehead BTP measurements, where no significant difference between men and women was identified. This difference in Bulk BTP Amplitude between the sexes might be attributed to PP as a confounding variable, as men were found to have significantly higher PP than women across all ages ($p < 0.001$), see Figure 7.

The final model was able to account for 11% of the variability in log(Bulk BTP Amp. Fore.), and 21% of the variability in log(Bulk BTP Amp. Temp.). Relationships between Bulk BTP Amplitude, PP, Age, and Sex are presented graphically in Figure 7.

Discussion

Transcranial Doppler (TCD) ultrasound has been used for many years for measuring blood flow through the major arteries (Aaslid et al. 1982). However, TCD for measurements of blood flow requires the skill and experience of a trained operator and is unsuitable for a high proportion of patients due to difficulty in obtaining measurements through the skull (Naqvi et al. 2013). As TCTD measures ultrasound backscatter from dense tissue rather than echoes from red blood cells suspended in an anechoic plasma, the received ultrasound signal from tissue is stronger than from blood, due to the higher density of scatterers available. TCTD measurements are also much easier to obtain than conventional TCD, as there is no need to orient the beam to coincide with a particular vessel location. BTP signals have been successfully obtained in all participants we have studied to date. Therefore, TCTD may prove to be a clinically useful addition to TCD by providing complementary tissue motion

estimates. This initial study investigated BTPs in a large cross-section of healthy subjects. Our findings show that BTP Amplitude varies considerably between hemispheres and between subjects in healthy participants, and is skewed towards lower values.

Insights into the characteristics of healthy BTPs gained using TCTD may help to improve our understanding of factors affecting brain tissue pulsatility. In this study we provide reference data from healthy volunteers, to be used for comparison with patient data in future research. The aim of this study was to better understand factors affecting Bulk BTP Amplitude in healthy subjects. Importantly, we confirm that good quality BTP data can be obtained from all participants from both the temporal and forehead positions. A small number of recordings were excluded from analysis due to the presence of artefacts rather than the absence of a signal. BTP amplitude was found to depend on probe position and sample depth, and to differ between hemispheres. A correlation between Bulk BTP Amplitude and PP was confirmed, and potential for a weaker influence of Age and Sex on Bulk BTP Amplitude was also indicated.

Our study concurs with previous MRI measurements by Weaver et al. (2012), describing increases in pulsation amplitude with proximity to the circle of Willis. BTP Amplitude measured through the skull increased with sample depth. Weaver et al. examined 6 subjects and found that the tissue surrounding the circle of Willis pulsates with an amplitude of approximately 150 μm. In our study, the highest reading obtained was 156 μm from a depth of 76 mm. Superficial brain tissue was found to pulsate at an amplitude of 10 μm in Weaver's study, which is similar to the median BTP Amplitude found in our study of 10.4 μm [IQR: 7.2, 14.6] for the forehead position and 5.2 μm [IQR: 3.4, 7.6] for the temporal position at the shallowest depth of 22 mm. However, the ultrasound beam profile displayed in Figure 1 will likely be distorted and attenuated in the presence of real skull, as shown by Evans and Gittins (2005); and the distortion will also vary between individuals,

386 therefore in this study we are unable to determine which brain structures are truly being
387 measured. As our measurements were not corrected for Doppler angle, it should be
388 remembered that our estimates reflect the component of tissue motion in the direction of the
389 beam, which is likely to slightly underestimate the true velocities and displacement of brain
390 tissue.

391 The TCD system used to acquire BTP data for this study was designed for blood flow
392 measurements and not optimised for BTP measurement. For example, our recordings were
393 limited to 8 seconds of data, and there was no user display for BTP visualisation. A system
394 capable of making continuous BTP recordings would be useful for future investigation of the
395 effects of PP, MAP, cerebral blood flow, CO_2, and inter-hemispheric differences on BTP
396 waveform shape and amplitude in physiological measurement studies. A system capable of
397 taking longer recordings would also allow for the rate of respiration to be considered, which
398 would be beneficial in selecting an accurate respiration filter cut-off, which is currently set at
399 75% of the mean cardiac frequency due to the assumption that the rate of respiration is much
400 slower than the normal resting heart rate. It may also be beneficial to extend the age range
401 and other characteristics of our healthy cohort to octogenarians and to perform a subgroup
402 analysis investigating participants with specific risk factors, e.g. hypertension and diabetes.
403 Although we aimed to attract healthy participants, some of the subjects recruited to our study
404 may have had undiagnosed underlying health conditions.

405 There is also opportunity to advance understanding of brain tissue motion using new
406 Doppler capabilities offered by high framerate ultrasound imaging. Echocardiography studies
407 have shown that using high framerate ultrasound gives more information on cardiac tissue
408 motion during early and late systole (Brekke et al. 2014). This could be applied to future
409 studies into brain tissue motion to achieve a greater temporal resolution, and therefore, a
410 more in-depth understanding on how brain tissue moves over the cardiac cycle. This study is

limited by the assumption that tissue strain is in one dimension (in the direction of the beam), whereas previous MRI studies have suggested that brain tissue moves in an inward and downward motion with each heartbeat (Greitz et al. 1992). It would be of interest to improve this technique by using vector Doppler ultrasound to estimate the magnitude and direction of tissue motion. Another technique that could be considered is time reversal transcranial ultrasound, which is a method that could be used to avoid aberration of the skull, as mentioned previously.

Overall, this study has confirmed that transcranial tissue Doppler ultrasound is capable of measuring brain tissue pulsations in human subjects. Overall, 5% of 8 second recordings were excluded due to artefacts. Our results provide insights into how BTPs vary amongst individuals, and have allowed us to develop a preliminary model of healthy Bulk BTP Amplitude as a function of PP, Age, and Sex. If BTPs are sensitive to pathophysiology, TCTD may be useful for distinguishing between healthy and pathological brain tissue motion.

Acknowledgements

We acknowledge Nihon Kohden (Japan) for donating the TCD and ECG monitoring equipment used in this study. We also acknowledge M. Moehring and A. Dewaraja (Broadview Laboratories, USA) for enabling data extraction from the TCD system for TCTD analysis, and K. Ebirim (Department of Engineering, University of Leicester, UK) for development of software to analyse BTP signals. We also thank Cloudcall (Leicester), Leicester U3A, and our staff and students for their participation in this research. This study was funded by the Science and Technology Facilities Council (STFC).

Table #1

Model coefficients, 95% confidence intervals, and p-values for each of the variables included in our preferred final regression model. The corresponding R^2 values are also displayed. The overall p-value for the model was $p < 0.001$.

Outcomes	Variable	Coefficient (95% CI)	p-value	R^2 value
log(Bulk BTP Amp. Fore.)	Constant	0.198 (-0.527, 0.923)	0.59	11.3%
	log(PP)	0.753 (0.277, 1.229)	$< 10^{-3}$	
	Age	-0.004 (-0.006, -0.001)	$< 10^{-3}$	
	Sex	-0.045 (-0.129, 0.040)	0.30	
log(Bulk BTP Amp. Temp.)	Constant	-0.090 (-0.793, 0.612)	0.80	20.6%
	log(PP)	0.597 (0.136, 1.058)	0.01	
	Age	0.001 (-0.002, 0.003)	0.44	
	Sex	0.110 (0.028, 0.192)	0.01	

References

Aaslid R, Markwalder TM, and Nornes H. Noninvasive transcranial doppler ultrasound recording of flow velocity in basal cerebral arteries. *J. Neurosurg*. 1982;57(6):769–774.

Biogeau J, Desmidt T, Dujardin PA, Ternifi R, Eudo C, Vierron E, Réméniéras JP, Patat F, Camus V, and Constans T. Ultrasound tissue pulsatility imaging suggests impairment in global brain pulsatility and small vessels in elderly patients with orthostatic hypotension. *J. Stroke and Cerebrovasc. Dis.* 2017;26(2):246–251.

Brekke B, Nilsen LCL, Lund J, Torp H, Bjastad T, Amundsen BH, Stoylen A, Aase SA. Ultra-high Frame Rate Tissue Doppler Imaging. *Ultrasound Med. Biol.* 2014;40(1):222-231.

Desmidt T, Hachemi ME, Réméniéras JP, Lecomte P, Ferreira-Maldent N, Patat F, and Camus V. Ultrasound brain tissue pulsatility is decreased in middle aged and elderly type 2 diabetic patients with depression. *Psychiatry Res. Neuroimaging*, 2011;193(1):63–64.

Desmidt T, Brizard B, Dujardin PA, Ternifi R, Réméniéras JP, Patat F, Andersson F, Cottier JP, Vierron E, Gissot V, Kim K, Aizenstein H, El-Hage W, and Camus V. Brain tissue pulsatility is increased in midlife depression: a comparative study using ultrasound pulsatility imaging. *Neuropsychopharmacology*, 2017;42(13):2575–82.

Evans DH and Gittins J. Limits of uncertainty in measured values of embolus-to-blood ratios in dual-frequency TCD recordings due to nonidentical sample volume shapes. *Ultrasound Med. Biol.* 2005;31(2):233-42.

Greitz D, Wirestam R, Franck A, Nordell B, Thomsen C, and Ståhlberg F. Pulsatile brain movement and associated hydrodynamics studied by magnetic resonance phase imaging. *Neuroradiology*. 1992;34:370–380.

Hoeks APG, Brands PJ, Arts TGJ, and Reneman RS. Subsample volume processing of doppler ultrasound signals. *Ultrasound Med. Biol.* 1994;20(9):953–65.

Ince J, Alharbi M, Minhas JS, and Chung EML. Ultrasound measurement of brain tissue movement in humans: A systematic review. *Ultrasound*. 2020;28(2):70-81.

Jurkonis R, Makũnaitė M, Baranauskas M, Lukoševičius A, Sakalauskas A, Matijošaitis V, and Rastenytė D. Quantification of endogenous brain tissue displacement imaging by radiofrequency ultrasound. *Diagnostics*. 2020;10:57.

Kucewicz JC, Dunmire B, Leotta DF, Panagiotides H, Paun M, and Beach KW. Functional tissue pulsatility imaging of the brain during visual stimulation. *Ultrasound Med. Biol.* 2007;33:681–690.

Kucewicz JC, Dunmire B, Giardino ND, Leotta DF, Paun M, Dager SR, and Beach KW. Tissue Pulsatitlity Imaging of Cerebral Vasoreactivity During Hyperventilation. *Ultrasound Med. Biol.* 2008;34(8):1200-8.

Mosher CP, Wei Y, Kamiński J, Nandi A, Mamelak AN, Anastassiou CA, Rutishauser U. Cellular classes in the human brain revealed in vivo by heartbeat-related modulation of the extracellular action potential waveform. *Cell Reports*. 2020;30:3536-51.

Naqvi J, Yap KH, Ahmad G, and Ghosh J. Transcranial doppler ultrasound: A review of the physical principles and major applications in critical care. *Int. J. Vasc. Med*. 2013;2013:13.

Ommen SR, Nishimura RA, Appleton CP, Miller FA, Oh JK, Redfield MM, and Tajik AJ. Clinical utility of doppler echocardiography and tissue doppler imaging in the estimation of left ventricular filling pressures: A comparative simultaneous doppler-catheterization study. *Circulation*, 2000;102:1788–1794.

Peixoto JL. Hierarchical variable selection in polynomial regression models. *Am. Stat.* 1987;41(4):311–313.

Siragusa MA, Brizard B, Dujardin P-A, Réméniéras JP, Patat F, Gissot V, Camus V, Belzung C, El-Hage W, Wosch T, Desmidt T. When classical music relaxes the brain: An experimental study using ultrasound brain tissue pulsatility imaging. *Int. J. Psychophysiol*. 2020;150:29-36.

Terem I, Ni WW, Goubran M, Salmani Rahimi M, Zaharchuk G, Yeom KW, Moseley ME, Kurt M, and Holdsworth SJ. Revealing sub-voxel motions of brain tissue using phase-based amplified MRI (aMRI). *Magn. Reson. Med.* 2018;80(6):2549–59.

Ternifi R, Cazals X, Desmidt T, Andersson F, Camus V, Cottier J-P, et al. Ultrasound measurements of brain tissue pulsatility correlate with the volume of MRI white-matter hyperintensity. *J Cereb. Blood Flow Metab*. 2014;34:942–4.

Weaver JB, Pattison AJ, McGarry MD, Perreard IM, Swienckowski JG, Eskey CJ, Lollis SS, and Paulsen KD. Brain mechanical property measurement using MRE with intrinsic activation. *Phys. Med. Biol.* 2012;57(22):7275–7287.

Figure captions

Fig. 1. Beam plot and equipment setup. (a) The path of the ultrasound beam superimposed on a resampled MR image showing brain anatomy. (b) Close-up of a free-field beam plot displaying normalised intensity along the direction of the beam. The Full Width Half Maximum (FWHM) is provided for 3 depths, showing how beam width varies along the ultrasound beam path. (c) A summary of the TCTD equipment setup. N.B. The free-field beam plot shown in (a) and (b) is only indicative, and does not fully represent the exact beam profile during the recording, due to changes in beam shape and direction after passing through the skull.

Fig. 2. Examples of BTP signals and illustration of tissue motion. Signals showing brain tissue motion for each 8 second recording presented as a waterfall plot; the shallowest depth of 22 mm is at the top of the figure, signals from successive depths are offset by 20 μm. (a) Shows an example of the largest pulsations of 156 μm, observed from a 23 year old male at the forehead on the right side, (b) provides a more typical example of a 15 μm pulsation from a 46 year old female measured from the forehead on the left side. BTP Amplitude was defined as shown schematically in (c) illustrating the direction of tissue motion, with upward blue arrows indicating outward tissue motion (toward the transducer), and downward red arrows indicating inward tissue motion (away from the transducer). The timing of BTPs, relative to the ECG waveform R-R interval, is indicated by the vertical lines in (a) and (b).

Fig. 3. Example of BTP waveform changes with brain anatomy. T1-weighted MR image from (a) a 22 year old male volunteer and (b) a 20 year old female volunteer. For reference, the Doppler gates are superimposed as white lines from 22 to 80 mm in depth, using the indicative beam path shown in Figure 1. BTP Amplitude is displayed for each of the 30

depths in the middle panels. The right side panel shows BTP signals as a waterfall plot, with signals from adjacent depths offset by 20 μm.

Fig. 4. Difference in Bulk BTP Amplitude between the right and left hemispheres. (a) shows right amplitudes minus left amplitudes for the forehead positions (96 subjects) and (b) shows temporal positions (97 subjects). The majority of subjects had higher right side pulsations (n = 57 for the forehead position, and n = 55 for the temporal position).

Fig. 5. Representative Bulk BTP waveforms over the cardiac cycle. (a) shows forehead positions (201 left and right recordings) and (b) shows temporal positions (204 left and right recordings). The line shows the median TCTD waveform, with error bars to indicate the IQR. This representative waveform has been obtained by averaging the BTP signal vertically over 30 gates, and where applicable, in time over multiple cardiac cycles.

Fig. 6. BTP changes with sample depth. Median BTP Amplitude and IQR (error bars), observed from (a) the forehead positions (201 left and right recordings) and (b) the temporal positions (204 left and right recordings). BTP Amplitudes were significantly larger and more varied when measured through the forehead. The IQR also increased with depth, suggesting greater variability in measurements at depth.

Fig. 7. Bulk BTP Amplitude changes with PP, Sex, and Age. Graphs for the forehead and temporal position, with both Bulk BTP Amplitude and PP displayed using a logarithmic scale. Graphs (a) and (b) show variations with PP, and (c) and (d) show how Bulk BTP Amplitude varies with Age. Men and women are indicated by hollow and filled markers, respectively.

Figure 1

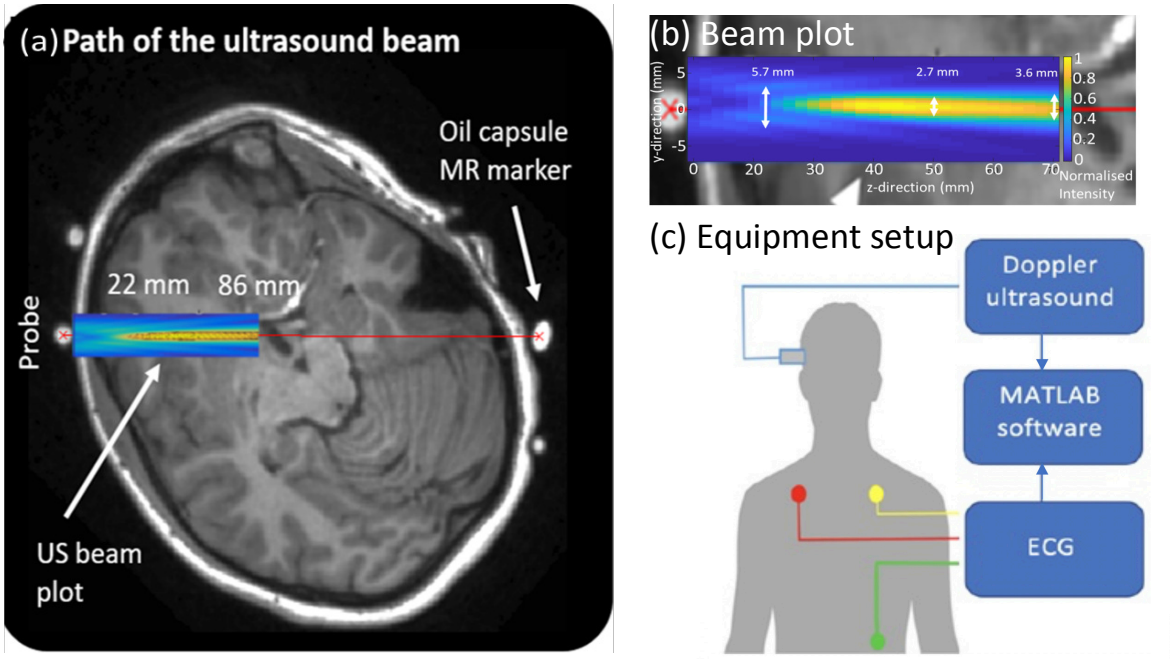

Figure 2

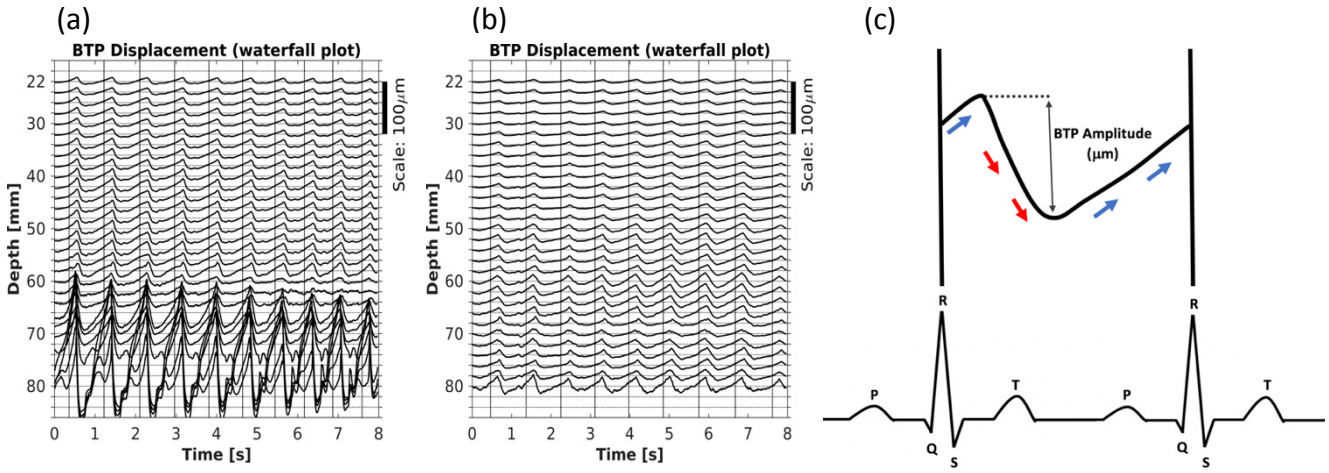

Figure 3

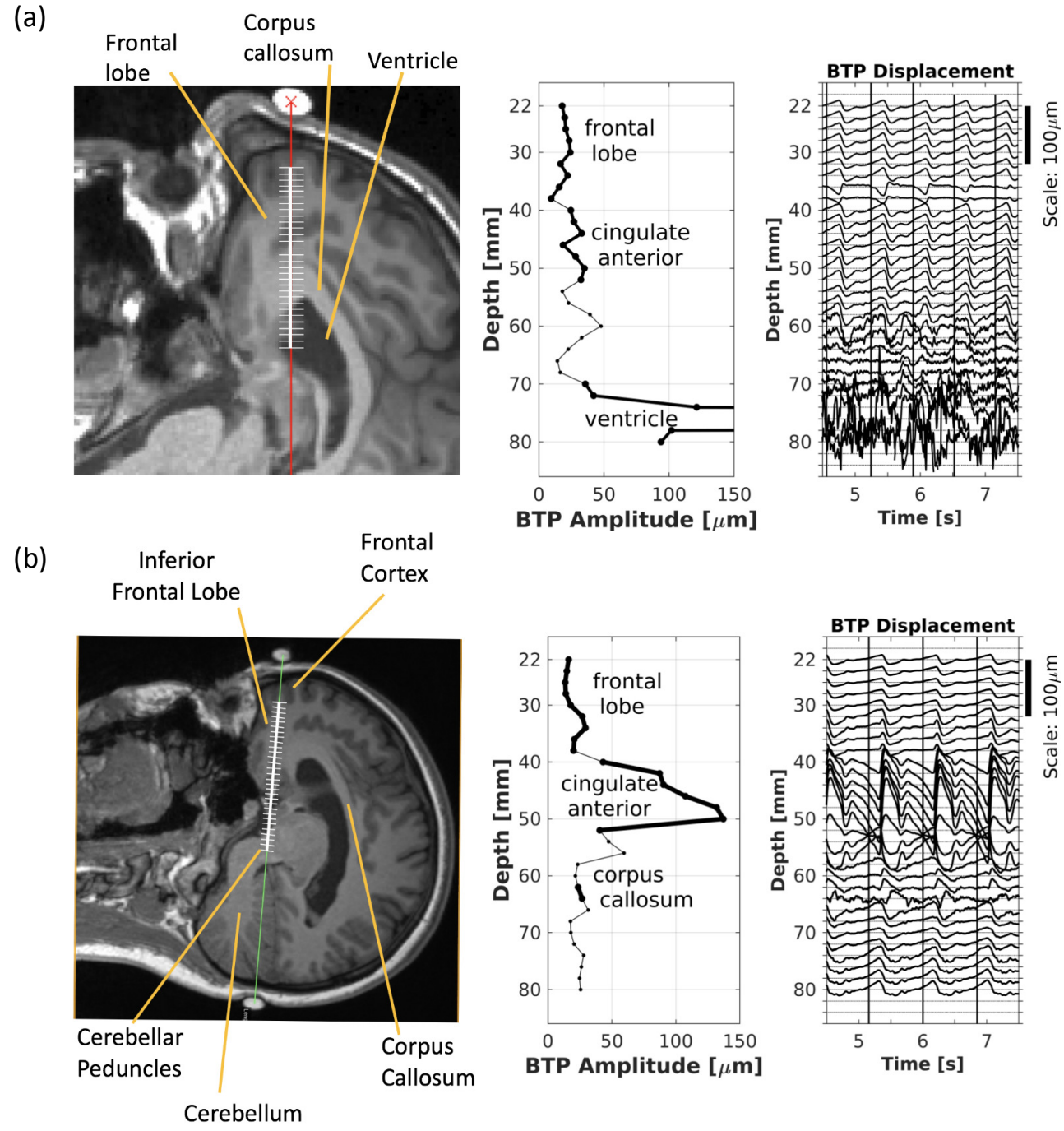
(a)
Frontal lobe
Corpus callosum
Ventricle
frontal lobe
cingulate anterior
ventricle
Depth [mm]
BTP Amplitude [μm]
BTP Displacement
Scale: 100μm
Time [s]
(b)
Inferior Frontal Lobe
Frontal Cortex
Cerebellar Peduncles
Cerebellum
Corpus Callosum
frontal lobe
cingulate anterior
corpus callosum

Figure 4

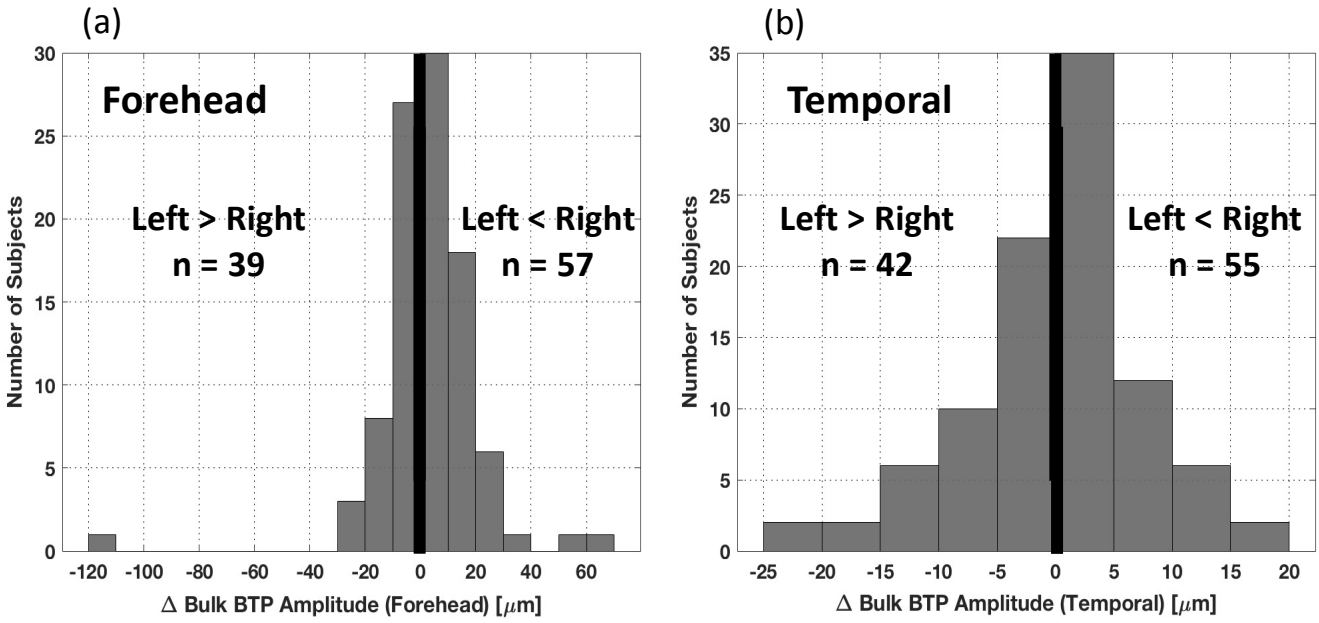

Figure 5

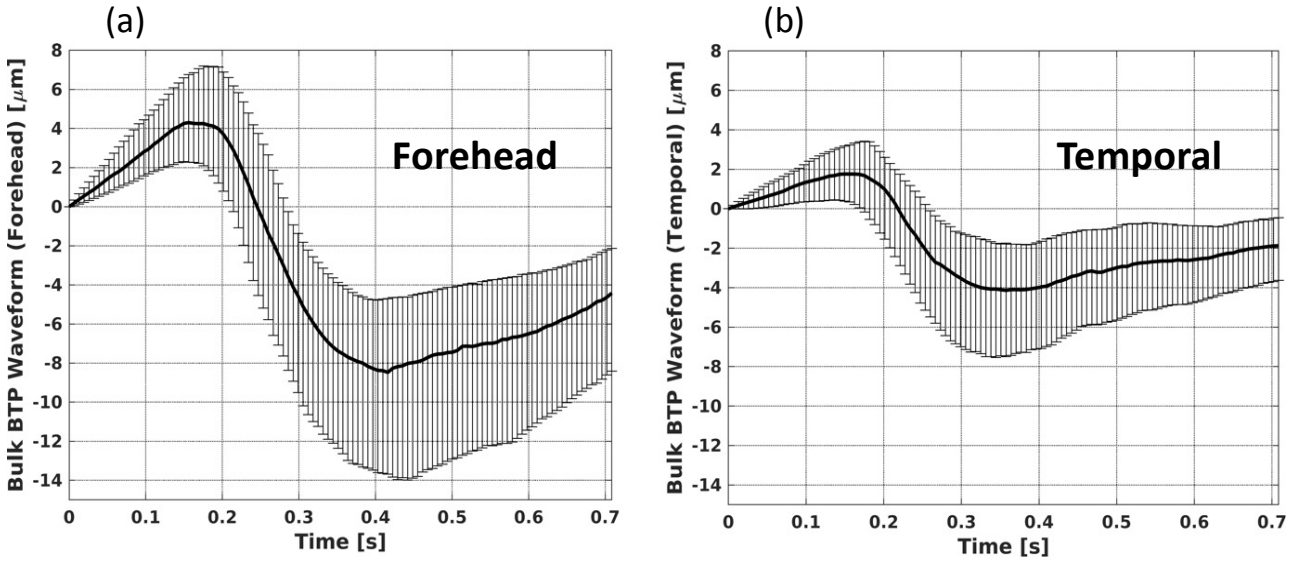

Figure 6

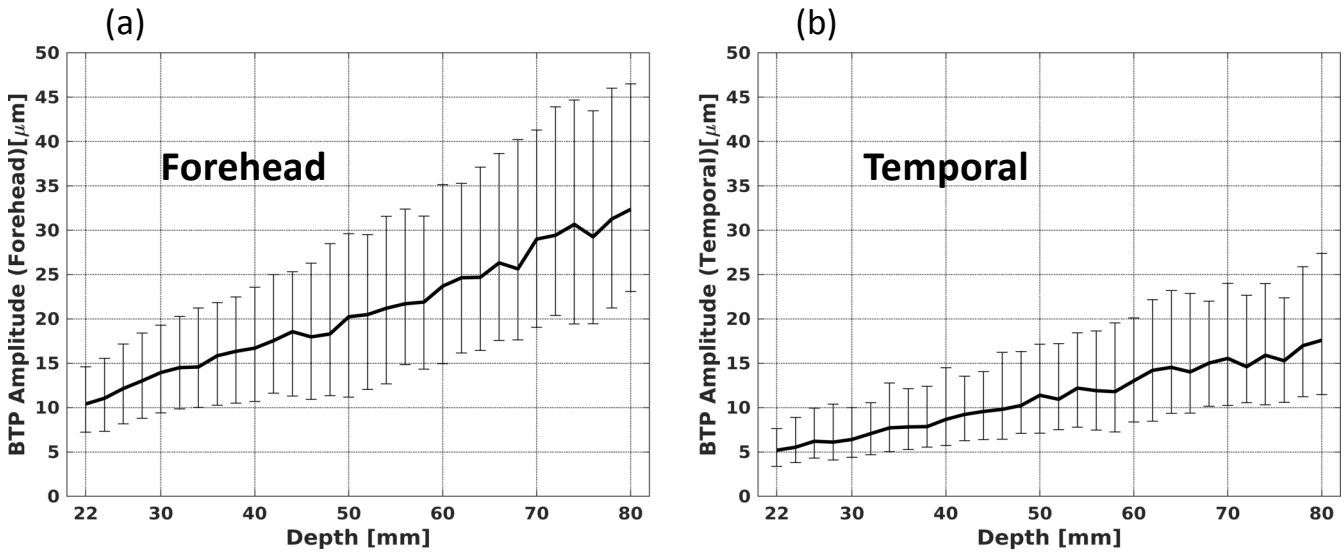

Figure 7